Ocean Modelling 48 (2012) 45–54

Contents lists available at SciVerse ScienceDirect

Ocean Modelling

journal homepage: www.elsevier.com/locate/ocemod

# Inclusion of a katabatic wind correction in a coarse-resolution global coupled climate model

Antoine Barthélemy *, Hugues Goosse, Pierre Mathiot, Thierry Fichefet

*Georges Lemaître Centre for Earth and Climate Research, Earth and Life Institute, Université catholique de Louvain, Louvain-la-Neuve, Belgium*

ARTICLE INFO

*Article history:*
Received 2 January 2012
Received in revised form 28 February 2012
Accepted 6 March 2012
Available online 14 March 2012

*Keywords:*
Katabatic winds
Sea ice
Antarctic
Southern Ocean
Deep water
Climate model

ABSTRACT

A correction for katabatic winds and polar easterlies is developed to deal with their dramatic underestimation by the atmospheric component of a coarse-resolution global coupled climate model. This correction relies on a comparison of the atmospheric surface circulation simulated by the model with the one provided by a regional atmospheric model, and consists of wind stress modifications in the vicinity of the Antarctic coast. Corrections are spatially varying and different for both wind components. The impacts of the correction on the modelled Antarctic sea ice and World Ocean's properties on long timescales are assessed, showing that katabatic winds thin sea ice and strongly enhance its production along the continent. Consequently, the formation rate, salinity and temperature of the Antarctic Bottom Water are increased. This leads to model results in better agreement with observations, especially in the deep ocean where the mean errors in temperature and salinity decrease by 9% and 37%, respectively. Hence, correcting katabatic winds seems to be an appropriate way to improve the representation of sea ice-related surface processes around Antarctica.



## 1. Introduction

Katabatic winds are amongst the most intensively studied features of the Antarctic climate. Their origin lies in the negative radiative budget of the dome-shaped ice sheet surface, which causes air masses to get cold and dense enough to flow downslope towards the coast, especially in winter. Topographically induced confluence zones are responsible for the strength and the persistence of the katabatic flow in several narrow zones near the coastal margin (Parish, 1988).

In such zones and in conjunction with barriers blocking the drift of sea ice (such as capes, islands or glacier tongues), katabatic winds are able to open coastal latent heat polynyas (Bromwich and Kurtz, 1984; Zwally et al., 1985; Adolphs and Wendler, 1995; Massom et al., 1998), i.e. large open water areas within the ice pack, from which newly formed ice is blown away. Among the 28 coastal polynyas listed along East Antarctica by Massom et al. (1998), 18 are at least partly forced by katabatic winds. These ice-free areas undergo intense heat losses to the atmosphere (Maykut, 1978), which promote high ice production rates. The subsequent brine rejection affects the stability of the water column, possibly leading to ocean convection and vertical mixing (Morales Maqueda et al., 2004).

The sinking of high density waters formed and accumulated on the continental shelf as a result of brine release has long been identified as one of the major mechanisms of Antarctic Bottom Water (AABW) production in the Weddell Sea (Gill, 1973). However, similar processes seem to be occurring in the Ross Sea and along the east coast of Antarctica (Jacobs, 2004; Williams et al., 2010). As a consequence, a poor representation of high latitude surface processes in global ocean general circulation models can induce large biases in the modelled deep ocean properties (Kim and Stössel, 1998; Goosse and Fichefet, 1999).

To overcome this problem in ocean circulation models, it has been proposed to restore the surface salinity towards observed climatologies (e.g., Toggweiler and Samuels, 1995) or to enhance the surface salinity to ad hoc higher values in specific regions around Antarctica (e.g., England, 1992, 1993). Nevertheless, this is thought to improve model results for wrong physical reasons and to distort the processes of deep water formation (Toggweiler and Samuels, 1995). Moreover, these approaches are inadequate for an accurate modelling of important biological and $CO_2$ exchange processes that are concentrated in polynya regions (e.g., Long et al., 2011). Another common practice to improve the deep ocean ventilation or the deep water formation in coarse-resolution ocean models is the carving of the topography. This method also lacks any physical justification.

In coupled sea ice–ocean models, the interactions between sea ice and ocean responsible for the production of high salinity shelf

* Corresponding author. Address: Georges Lemaître Centre for Earth and Climate Research, Earth and Life Institute, chemin du Cyclotron 2, Box L7.01.11, B-1348 Louvain-la-Neuve, Belgium. Tel.: +32 10 47 32 70; fax: +32 10 47 47 22.

*E-mail addresses:* antoine.barthelemy@uclouvain.be (A. Barthélemy), hugues.goosse@uclouvain.be (H. Goosse), pierre.mathiot@uclouvain.be (P. Mathiot), thierry.fichefet@uclouvain.be (T. Fichefet).

1463-5003/$ - see front matter © 2012 Elsevier Ltd. All rights reserved.
http://dx.doi.org/10.1016/j.ocemod.2012.03.002

waters are explicitly represented, but other difficulties arise from the lack of strong katabatic winds in the atmospheric forcings generally used to drive them (e.g., Stössel et al., 2011). The resolution of global atmospheric general circulation models and reanalyses is indeed insufficient to account for the local topographic variations that largely influence the katabatic flow (Jourdain and Gallée, 2011). To tackle this issue in the ERA40 global reanalysis (Uppala et al., 2005), Mathiot et al. (2010) developed a local correction of the winds in the vicinity of Antarctica, based on a comparison between the low-level circulation in the reanalysis and the one simulated by a regional atmospheric model. They applied this correction in a relatively high-resolution global ocean-sea ice model, focussing on the improvement in the representation of water mass properties on the continental shelf in a 44-year simulation spanning the period 1958–2001.

In order to complement this work, the present study aims at studying the sea ice and deep ocean long-term response to the introduction of a katabatic wind correction. To perform the thousand year long simulations required for such an analysis, the Earth system model of intermediate complexity LOVECLIM is an appropriate tool, as it is much faster than the one used in Mathiot et al. (2010). Furthermore, since LOVECLIM is a coupled model, it is able to represent the interactions between atmosphere and ocean. A correction similar to the one proposed by Mathiot et al. (2010) is first developed for LOVECLIM. Two simulations are then performed, including or not the new katabatic wind correction, in order to assess its effects on sea ice and the World Ocean.

The paper is organised as follows. The LOVECLIM model, the katabatic wind correction and the experimental design are described in Section 2. Results are presented and discussed in Section 3. We first deal with the effects of the correction on sea ice, then we consider its impacts on the ocean. A summary of our findings and concluding remarks are finally given in Section 4.

## 2. Methodology

### 2.1. The LOVECLIM model

LOVECLIM is a three-dimensional Earth system model of intermediate complexity, described in detail in Goosse et al. (2010). In this study, we use version 1.2 of this model without interactive ice sheet and ocean carbon cycle components. The atmospheric component is ECBilt (Opsteegh et al., 1998), a T21, quasi-geostrophic model, with three vertical levels at 800 hPa, 500 hPa and 200 hPa. In the physical space, the corresponding grid resolution is about 5.6° in latitude and longitude. The ocean is represented by CLIO (Goosse and Fichefet, 1999), which consists of an ocean general circulation model coupled to a comprehensive thermodynamic–dynamic sea ice model, with a horizontal resolution of 3° by 3°. The vertical discretization follows the simple so-called "z-coordinate", and there are 20 vertical levels in the ocean, with depths ranging from 10 m at the surface to 750 m close to the bottom. ECBilt and CLIO are further coupled to the VECODE land surface model (Brovkin et al., 2002) that simulates the vegetation dynamics.

### 2.2. Low-level circulation around Antarctica

The atmospheric surface circulation off Antarctica is characterised by two major features. Firstly, strong katabatic winds blow offshore in the coastal areas situated downstream of topographically induced confluence zones. Those winds lose their dynamical support when they reach the nearly horizontal ice shelves or the ocean, but they can extend over a few tens of kilometers offshore (Bromwich and Kurtz, 1984; Adolphs and Wendler, 1995). They are thus able to interact with sea ice to create coastal polynyas.

The second feature of the low-level circulation is polar easterlies, blowing at an average latitude of 66° S. Easterlies are mainly due to the low pressure band surrounding the continent (King and Turner, 1997), but are also supported by the deflection of the katabatic flow to the left by the Coriolis force (Davis and McNider, 1997).

A comparison of the surface wind field simulated by LOVECLIM in the vicinity of Antarctica with the one simulated with the Modèle Atmosphérique Régional (MAR, see next section; Gallée and Schayes, 1994) reveals the deficiencies of LOVECLIM in the representation of coastal winds. The upper and centre panels of Fig. 1 show the mean meridional and zonal wind stress components simulated in September, i.e. when katabatic winds are strongest, by MAR between 1980 and 1989 and by LOVECLIM in a quasi-equilibrium run under preindustrial conditions. Offshore winds are dramatically too weak in LOVECLIM, except in the western part of the Ross Sea. Easterlies are better represented, though also underestimated along the continent. Both the coarse horizontal and vertical resolutions and the simplistic representation of the atmospheric boundary layer in LOVECLIM explain those biases in the simulation of coastal winds.

### 2.3. Correction of katabatic winds

Ocean modellers have proposed different corrections to face the issue of the katabatic wind underestimation in global atmospheric models and reanalyses. Kim and Stössel (1998) fix the (northward) meridional component of the wind velocity to 20 m $s^{-1}$ along the coast of East Antarctica, the Amundsen Sea and the Bellingshausen Sea, and to 10 m $s^{-1}$ elsewhere. Röske (2006) corrects the magnitude of the wind speed by an offset which is proportional to the difference between the wind velocity over sea and the wind velocity over land if the air temperature is below 0 °C. Mathiot et al. (2010) propose to apply a correction to both the meridional and zonal components of the wind velocity in the ERA40 atmospheric reanalysis, in the form of a positive scale factor deriving from a comparison of coastal winds in the reanalysis with the ones simulated by the regional model MAR. Our work is based on their method.

As observations are too sparse to provide a quantitative picture of the katabatic flow at the continental scale, the correction relies on a simulation performed with the regional model MAR, as discussed in Mathiot et al. (2010). This mesoscale, primitive-equation atmospheric model is fully described in Gallée and Schayes (1994). In addition to its fine horizontal (100 km) and vertical (10 m for the lowermost layer) resolutions, MAR has surface roughness length parameterizations specifically designed to provide a realistic low-level circulation. The simulated katabatic winds are indeed in good agreement with observations, as shown by Mathiot et al. (2010) and Jourdain and Gallée (2011).

Given the katabatic wind large spatial variability, the applied corrections must be local. As the CLIO resolution at 70° S is around 300 km by 100 km (in the meridional and zonal directions, respectively), the correction should only affect the ocean grid points adjacent to the coast. Also, because latent heat polynyas driven by katabatic winds are usually situated in the lee of features blocking drifting sea ice, both wind components must be corrected. For the sake of simplicity, our correction will neglect the seasonal cycle of the katabatic flow, and constant corrections are hence computed for the meridional and zonal wind stresses at each coastal point in the CLIO grid.

The quantitative comparison of the LOVECLIM and MAR surface wind fields is done as follows. We average the wind stresses simulated by LOVECLIM over the last 10 years of a 2000 year long

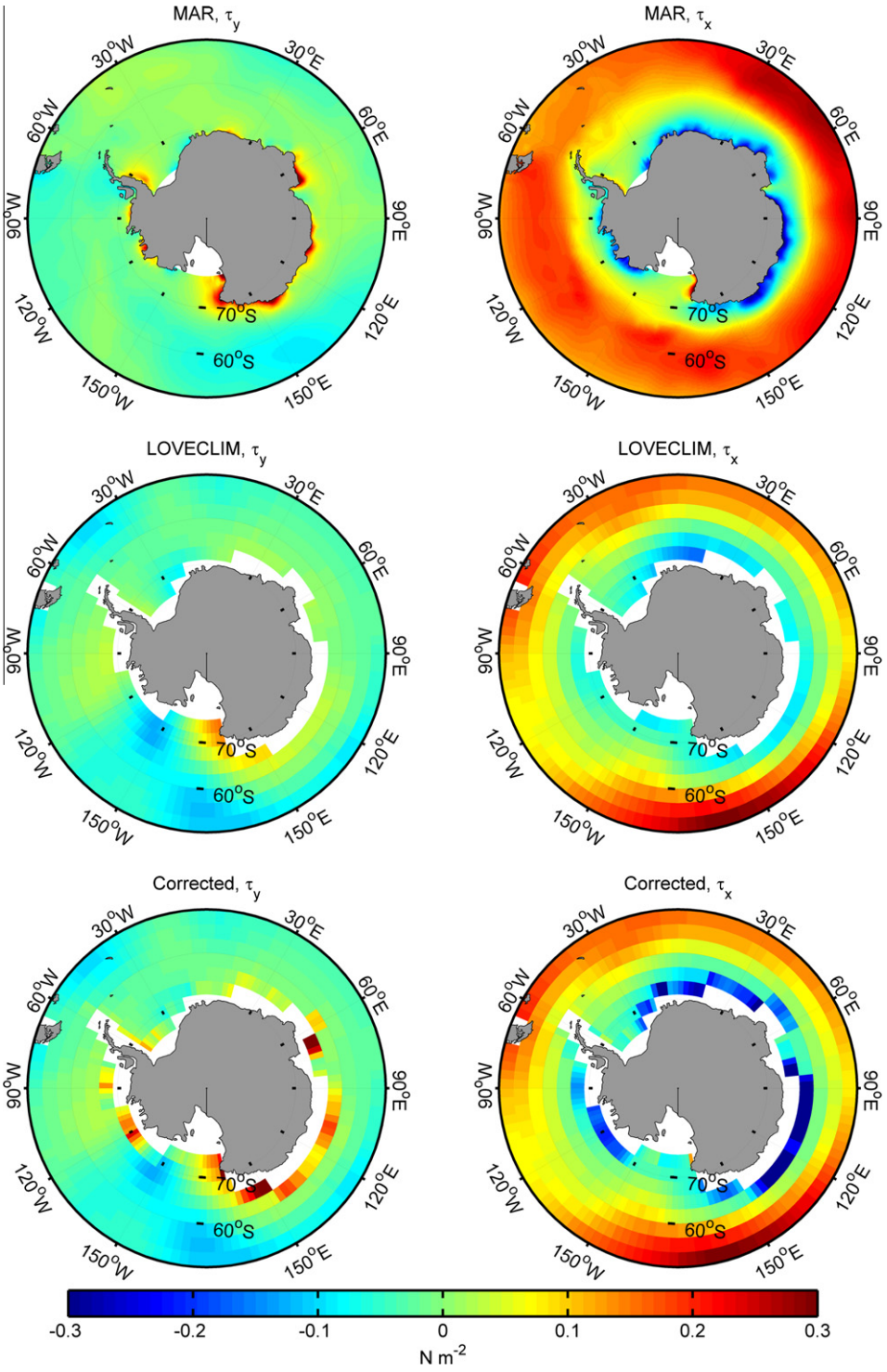


**Fig. 1.** September meridional ($\tau_y$, left) and zonal ($\tau_x$, right) wind stresses (in N m$^{-2}$), simulated by MAR (upper part) and LOVECLIM (centre part), and corrected along the coast as described in Section 2.3 (lower part).

quasi-equilibrium simulation under preindustrial conditions, as well as the wind stresses provided by MAR over the period 1980–1989. Thus the conditions slightly differ between MAR and LOVECLIM experiments, but differences in the simulated winds are essentially due to the models physics and resolutions. Besides, the corrections that we will derive will be specific to the present climate, therefore they should ideally be recalculated for use in past climate simulations or climate change scenarios. However, even for such simulations, the correction presented in this study is sufficient to provide a first order estimation of the effects of katabatic winds. After interpolating the MAR fields onto the CLIO grid, we compute, for each coastal point, the ratio of and the difference between both components of the annual mean wind stress. We introduce the following definitions:

$$\rho_y = \frac{\overline{\tau}_{y,\mathrm{MAR}}}{\overline{\tau}_{y,\mathrm{LOVECLIM}}}, \quad \rho_x = \frac{\overline{\tau}_{x,\mathrm{MAR}}}{\overline{\tau}_{x,\mathrm{LOVECLIM}}}, \tag{1}$$

$$\delta_y = \overline{\tau}_{y,\mathrm{MAR}} - \overline{\tau}_{y,\mathrm{LOVECLIM}}, \quad \delta_x = \overline{\tau}_{x,\mathrm{MAR}} - \overline{\tau}_{x,\mathrm{LOVECLIM}}, \tag{2}$$

**Table 1**
Corrections applied to the meridional (upper part) and zonal (lower part) wind stresses in LOVECLIM, along with the number of coastal points in each case. The total number of coastal points is 126. See Section 2.3 for the definitions of $\rho_y$, $\rho_x$, $\delta_y$ and $\delta_x$.

| Case | # Points | $\alpha$ | $\beta$ |
|---|---|---|---|
| $\rho_y < -6$ | 13 (10%) | 1 | $\delta_y$ |
| $-6 < \rho_y < 0$ | 21 (17%) | $\rho_y$ | 0 |
| $0 < \rho_y < 6$ | 66 (52%) | $\rho_y$ | 0 |
| $6 < \rho_y$ | 26 (21%) | 1 | $\delta_y$ |
| $\rho_x < -6$ | 2 (2%) | 1 | $\delta_x$ |
| $-6 < \rho_x < 0$ | 15 (12%) | 1 | 0 |
| $0 < \rho_x < 6$ | 105 (83%) | $\rho_x$ | 0 |
| $6 < \rho_x$ | 4 (3%) | 6 | 0 |

where the $\overline{\tau}$ are the annual mean wind stress components, with subscripts indicating the direction and the model. According to the value of $\rho_x$ and $\rho_y$, the wind stress correction takes the form of either a scale factor $\alpha$ or an offset in stress $\beta$. The various cases are listed in Table 1.

We first consider meridional wind stresses. If the absolute value of the ratio $\rho_y$ is smaller than 6, we apply a multiplicative correction $\alpha_y$, equal to $\rho_y$ itself. This increases the strength of the katabatic winds underestimated in LOVECLIM, and corrects their direction where $-6 < \rho_y < 0$. In order to insure the numerical stability of the ocean model, the scale factor $\alpha_y$, which will multiply the instantaneous wind stresses, is limited to a maximum value of 6. The latter is chosen according to the distribution of the ratios $\rho_x$ and $\rho_y$ at all coastal points, which shows an abrupt decline at a value of about 6. The points where $|\rho_y| > 6$ are located in regions where LOVECLIM winds are very weak while strong katabatic winds are present in MAR. As no proportionality can be deduced between the winds in the two models, the correction takes the form of an offset in wind stress $\beta_y$, equal to $\delta_y$.

The methodology applied for the zonal wind stresses for $0 < \rho_x < 6$ and $\rho_x < -6$ is the same as for the meridional ones, but it differs in the two other cases. First, no correction is applied where $-6 < \rho_x < 0$. This aims at avoiding spurious sea ice convergence or divergence zones along the coast, in places where the correction would change the direction of sea ice drift. The reasoning does not apply to the 2 points where $\rho_x < -6$, since these are situated along the west coasts of the Ross Sea and the Antarctic Peninsula, where zonal winds are actually offshore winds. Second, where $\rho_x > 6$, we use a scale factor $\alpha_x$ equal to 6, which only causes a slight underestimation of wind stresses at these few points in LOVECLIM compared to MAR.

When the katabatic wind correction is activated, the wind stresses calculated from the atmospheric component are modified, at each time step, as:

$$\tau_{y,\text{corrected}} = \alpha_y \tau_{y,\text{LOVECLIM}} + \beta_y, \quad (3)$$

and similarly in the zonal direction.

The lower panels of Fig. 1 show how the September wind field is corrected around Antarctica. In spite of the fact that corrections are constant in time, the seasonal cycle is relatively well approximated (not shown). In September, the intensity of coastal easterlies increases nearly everywhere. Katabatic winds appear as a patchy pattern, reflecting their high spatial variability. Particularly strong winds are encountered around 70° E and 150° E, but nearly all coastal regions undergo higher offshore winds. It should be noted, however, that the coarse resolution of CLIO allows representing only the gross features of the low-level circulation along the continent.

### 2.4. Experimental design

Two simulations are performed in order to evaluate the impact of the katabatic wind correction on sea ice and ocean. The first one corresponds to the standard configuration of LOVECLIM (Goosse et al., 2010) and is referred to as CTRL. The katabatic wind correction is activated in the second simulation, named KATA. Because we aim at studying the long-term response of the climate simulated by LOVECLIM, CTRL and KATA are 2000 year long quasi-equilibrium runs under preindustrial conditions, and we examine the outputs averaged over the last 100 years.

## 3. Results and discussion

The following discussion first deals with the changes in sea ice caused by the introduction of the katabatic wind correction in LOVECLIM. We will focus on the winter season, when sea ice is present along the whole Antarctic coast and when katabatic winds have their major impacts. Then, we consider the response of the Southern Ocean. Finally, we examine temperature and salinity changes in the World Ocean.

### 3.1. Sea ice

Sea ice concentration exhibits widespread changes in response to the introduction of katabatic winds. Fig. 2 shows the simulated concentration in September in the CTRL simulation and the difference between KATA and CTRL. Although the correction only acts along the coast, the most significant variations occur within the ice pack and along the ice edge, reaching ±50% in some areas. They are linked with oceanic processes discussed in Section 3.2. Along the continent, the decrease in sea ice concentration is rather limited. Moreover, the largest changes do not match the strongest katabatic winds. Our correction being based on the MAR wind fields smoothed and interpolated onto the CLIO grid, the resulting smoothed coastal winds are seemingly too weak to have a large impact on local ice concentration.

On the contrary, sea ice thickness experiences a much stronger response along Antarctica, reflecting the transport of ice by katabatic winds. When averaged over all the coastal ocean grid cells and over the winter season (from April to September), thickness decreases by 23%, while concentration is lower by only 6% (Table 2). Furthermore, in the case of thickness, the largest changes tend to occur in regions undergoing the most intense winds (Fig. 3). The thinning exceeds 1 m in several regions and reaches around 1.5 m close to 130° W, for instance. On the other hand, thickness is higher in the open ocean, where sea ice is advected.

The changes in total ice extent or volume in the Southern Hemisphere appear rather small. The winter mean total sea ice extent decreases by 3%, from $19.7 \times 10^6$ km$^2$ in CTRL to $19.1 \times 10^6$ km$^2$ in KATA. In September, the simulated sea ice edge is displaced northwards between 20° W and 80° E in KATA, a region where LOVECLIM underestimates the ice extent. The agreement between the model results and observations is however not significantly increased in the other regions, where the ice edge changes remain small.

As Antarctic coastal regions in the Southern Ocean are in contact with the coldest air masses, more than half of the ice volume produced in winter in the CTRL simulation is formed along the continent (Table 2), in regions only accounting for 24% of the mean sea ice extent in the considered period. When the katabatic wind correction is activated, this fraction of the ice produced in the first oceanic grid cells reaches 77%. The decrease in sea ice thickness (and, to a lesser extent, in sea ice concentration) allows enhanced heat losses to the atmosphere, and hence an increase in the ice production rate of 53%. It should be noted, however, that the additional $2.6 \times 10^3$ km$^3$ of sea ice produced along the coast exceeds the $0.9 \times 10^3$ km$^3$ increase in total ice volume produced, indicating

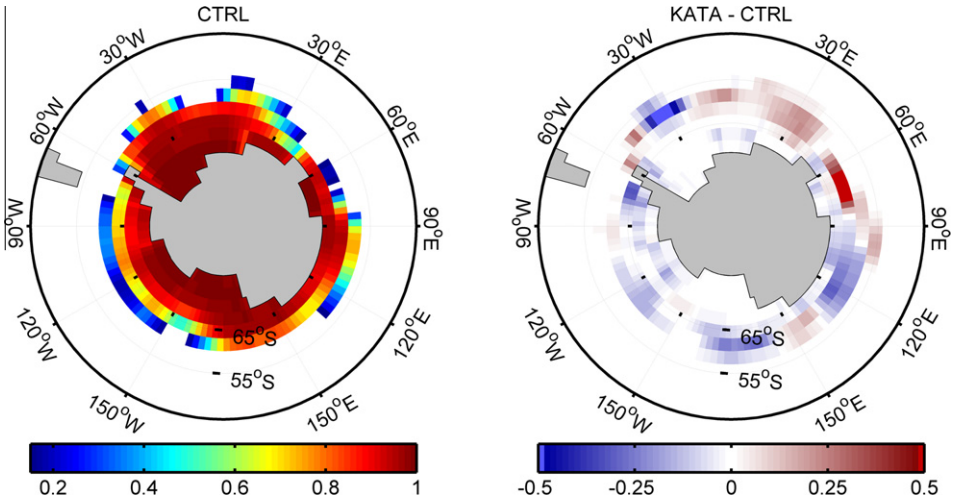


**Fig. 2.** Sea ice concentration in September, in CTRL (left) and the difference between the two simulations (KATA–CTRL, right). Red (blue) areas correspond to higher (lower) concentration in KATA. (For interpretation of the references to colour in this figure legend, the reader is referred to the web version of this article.)

**Table 2**
Winter mean properties and production of sea ice along the coast. Variables are averaged or cumulated over a period from April to September and over the coastal ocean grid cells around the whole Antarctica (except for the total volume produced and the total sea ice extent).

| Variable | CTRL | KATA |
|---|---|---|
| Concentration (%) | 88 | 83 |
| Thickness (m) | 1.04 | 0.80 |
| Production rate (m month$^{-1}$) | 0.18 | 0.27 |
| Volume produced ($10^3$ km$^3$) | 5.0 | 7.7 |
| Total volume produced ($10^3$ km$^3$) | 8.9 | 9.9 |
| Fraction of total volume produced along the coast (%) | 56 | 77 |
| Total sea ice extent ($10^6$ km$^2$) | 19.7 | 19.1 |

that the net production in the open ocean is lesser in KATA. Mathiot et al. (2010) obtained a similar result.

The annual sea ice production, defined as the ice produced minus the ice melted in one year in each grid cell, is presented in Fig. 4. In CTRL, production tends to concentrate in regions where winds and coastal configuration cause a divergence of the sea ice cover. The best example is the western part of the Ross Sea, where strong southerly winds are inducing an ice production of more than 4 m year$^{-1}$. Ice formed at high latitudes is then transported northwards and melts essentially between 65° S and 55° S, on an annual average.

The contrast between coastal regions and the open ocean is strengthened by the correction of coastal winds: both the coastal production and the open ocean melt increase in KATA. Higher production rates are encountered in places where ice divergence is more pronounced, because of particularly strong katabatic winds (e.g., 70° E, compare Figs. 1 and 4), of a combination of katabatic winds and easterlies (e.g., 120° W) or of easterlies only (e.g., 80° E). The increase in production exceeds 1 m year$^{-1}$ in numerous areas. As a result, the katabatic wind correction induces a significant enhancement in brine rejection along the coast, while the freshwater flux to the ocean increases in the open ocean.

### 3.2. Response of the Southern Ocean

In the ocean model CLIO, in addition to the turbulence closure scheme (Goosse et al., 1999), the vertical mixing due to convection

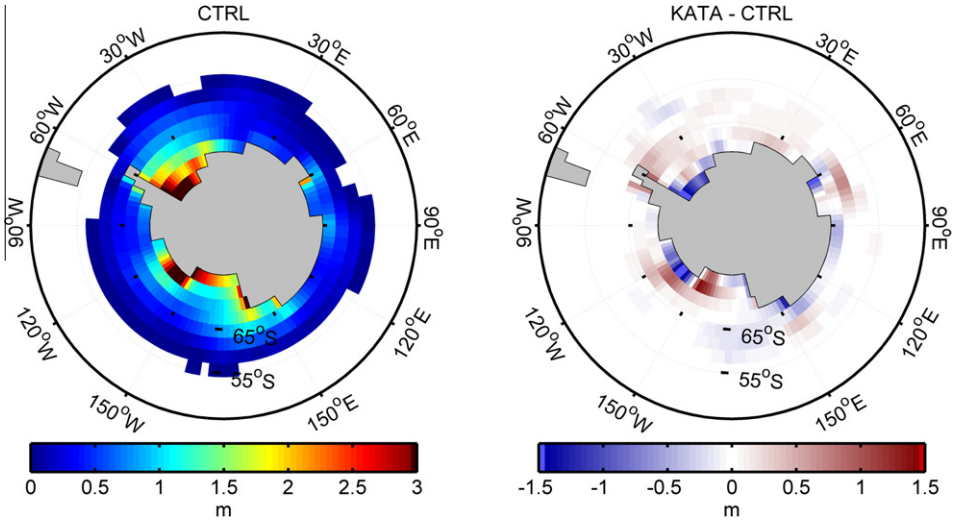


**Fig. 3.** Sea ice thickness in September, in CTRL (left) and the difference between the two simulations (KATA–CTRL, right). Red (blue) areas correspond to thicker (thinner) ice in KATA. (For interpretation of the references to colour in this figure legend, the reader is referred to the web version of this article.)

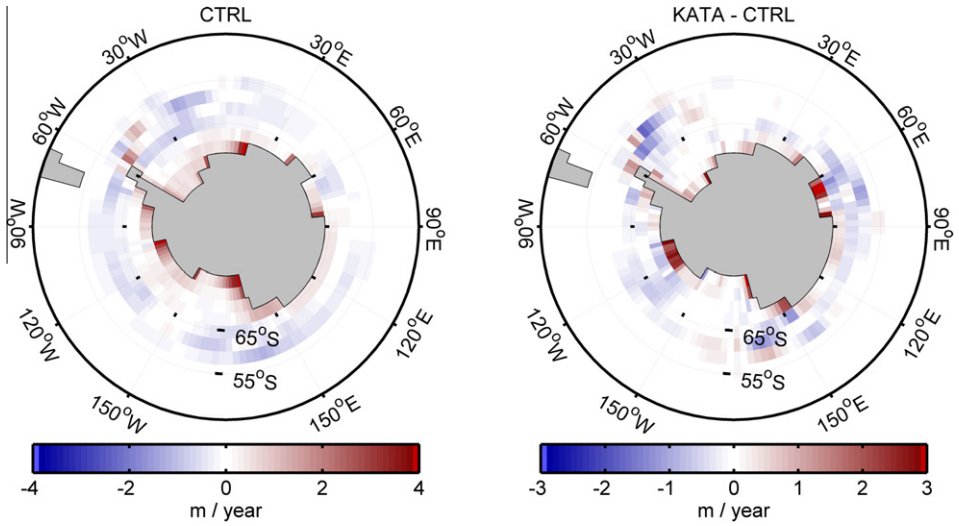


**Fig. 4.** Annual sea ice production (in m year$^{-1}$), in CTRL (left) and the difference between the two simulations (KATA–CTRL, right). For CTRL, red (blue) areas correspond to a net production (melt). For the difference, red (blue) areas correspond to higher (lower) production in KATA. (For interpretation of the references to colour in this figure legend, the reader is referred to the web version of this article.)

is represented through a convective adjustment scheme: when the water column is statically unstable on a vertical depth range greater than 100 m, the vertical diffusivity is increased to 10 m$^2$ s$^{-1}$. The depth of convection simulated in September is represented in Fig. 5. In the open ocean, the higher freshwater flux in KATA stabilizes the water column and hence results in a reduction of convection.

Along the coast, changes in convection are not linked with the amount of additional salt rejected, but rather depend on the presence of a continental shelf in the model. In coastal regions between 100° E and 140° E, the continental shelf is too narrow to be represented at the CLIO resolution. The slight increase in brine rejection in this area causes a dramatic deepening of the oceanic convection, reaching more than 400 m. When additional salt release takes place on the continental shelf, as it is the case in basically all other regions, such an enhancement in convection does not occur. Waters with higher salinity (typically 0.1 psu) actually accumulate on the shelf, particularly close to the bottom. The mean vertical density profile of the water column is consequently more stable, which prevents any strong deepening of the convection. In the southwestern part of the Ross Sea, on average, this even results in a somehow counter-intuitive reduction of the convection.

Sea surface temperature (SST) changes between KATA and CTRL are displayed in Fig. 6. Between 20° E and 80° E, the surface cooling is related to the decrease in vertical mixing. In the other regions, the variations in SST mostly arise from slight modifications in the path of the Antarctic Circumpolar Current (ACC). Because the ACC is approximatively in geostrophic equilibrium, these modifications are understood as a consequence of changes in salinity gradients, and hence in density gradients, in the Southern Ocean. The changes in the ACC path are responsible for large temperature changes, since the current is associated with large meridional temperature gradients (Orsi et al., 1995). The ACC shifts southwards and brings warmer waters closer to Antartica around 170° E, between 160° W and 120° W and around 30° W. Inversely, it is displaced northwards around 170° W and 50° W, and to a lesser extent between 80° E and 130° E, leading to an ocean cooling in those regions. The current also experiences a slight increase in strength, from 118.7 Sv through the Drake Passage in CTRL to 121.8 Sv in KATA.

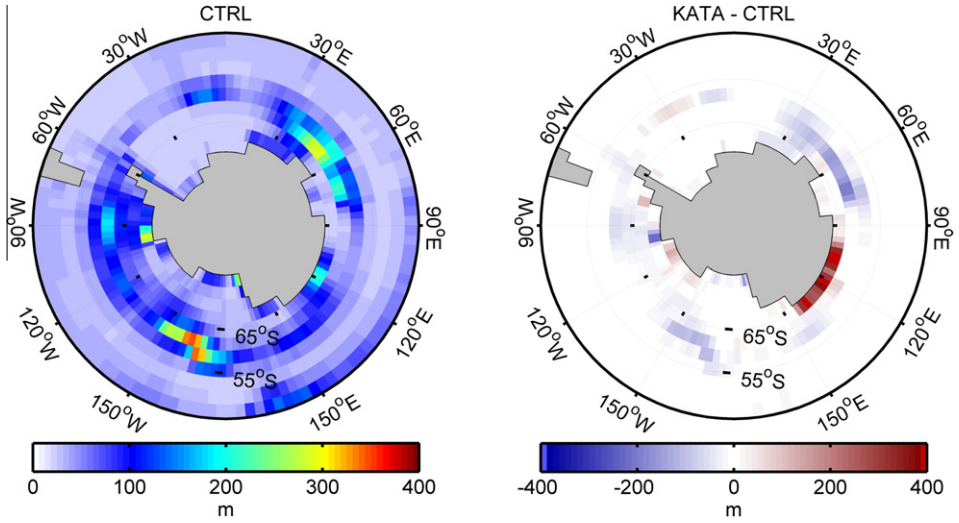


**Fig. 5.** Depth of convection (in m) in September, in CTRL (left) and the difference between the two simulations (KATA–CTRL, right). Red (blue) areas correspond to deeper (shallower) convection in KATA. (For interpretation of the references to colour in this figure legend, the reader is referred to the web version of this article.)

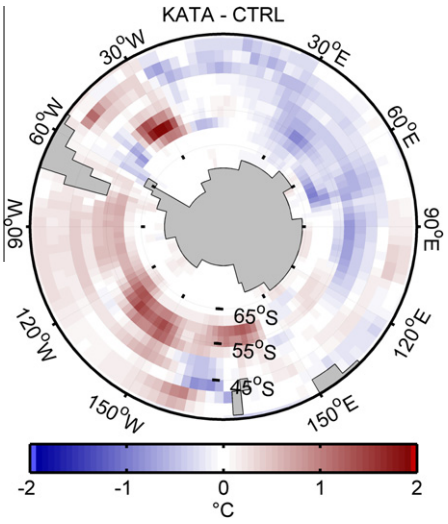


**Fig. 6.** Sea surface temperature difference (in °C) between the two simulations (KATA–CTRL), in September. Red (blue) areas correspond to higher (lower) surface temperature in KATA. (For interpretation of the references to colour in this figure legend, the reader is referred to the web version of this article.)

A comparison of Fig. 6 with Fig. 2 indicates that the major features of sea ice concentration changes are consistent with the variations in SST described above. However, the matching between concentration and surface temperature changes is lesser than between surface temperature changes and their suspected oceanic causes (i.e. ACC shifts and changes in vertical mixing). This suggests that SST changes have indeed an oceanic origin, rather than being caused by ice concentration variations combined with the albedo-temperature feedback. Besides, the role of the atmosphere appear limited. The latter slightly adjusts in response to oceanic changes, without significant large-scale feedbacks on the ocean (not shown).

The above-mentioned changes in ocean and sea ice result from the effects of katabatic winds on sea ice transport along the coast, rather than in direct effects on ocean dynamics. The present analysis has indeed been conducted with a version of the correction in which katabatic winds impact only sea ice transport (Barthélemy, 2011). Results were both qualitatively and quantitatively similar.

### 3.3. Large-scale temperature and salinity changes

Higher density (because of higher salinity) waters present at depth on the Antarctic continental shelf increase by 38% the downslope flow from the shelf (from 3.4 Sv to 4.7 Sv), which is parameterized following Campin and Goosse (1999) in LOVECLIM. The Antarctic Bottom Water (AABW) production (diagnosed as the maximum of the meridional overturning streamfunction in the Southern Ocean) is consequently enhanced, by 2.8 Sv, reaching 17.6 Sv in the KATA simulation. However, the export of AABW to the other basins remain unchanged. The circulation of the North Atlantic Deep Water (NADW) is also unaffected (Fig. 7).

Deep water properties are especially influenced by katabatic winds. Zonal averages of salinity changes between KATA and CTRL are shown in Fig. 8, along with a comparison between the CTRL simulation and the observational data from the World Ocean Atlas (Conkright et al., 2002). They are computed between 72° W and 24° E, between 24° E and 135° E and between 135° E and 72° W, corresponding approximatively to the Atlantic, the Indian and the Pacific sectors of the Southern Ocean, respectively.

Considering each oceanic basin separately reveals that changes are associated with an increase in the AABW salinity. Indeed, higher salinity is found in KATA in regions occupied by that water mass, that is the whole deep ocean in the Indian and Pacific sectors, but in the Atlantic sector only in the Southern Ocean close to the

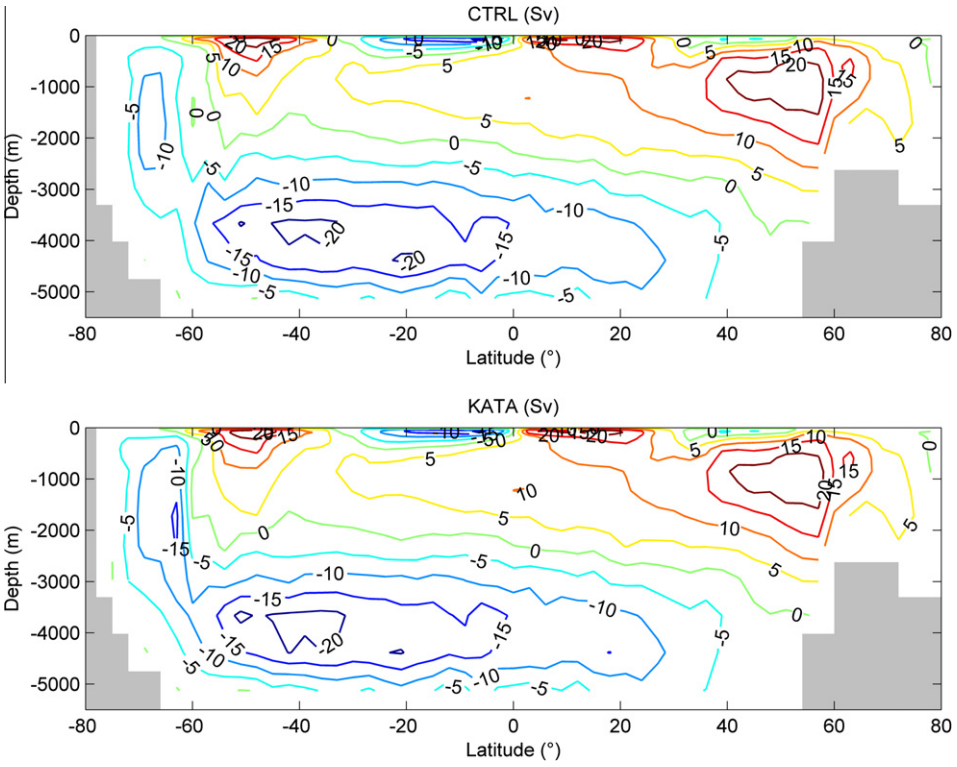


**Fig. 7.** Zonally integrated meridional streamfunction in the World Ocean, in CTRL (upper part) and KATA (lower part). The contour interval is 5 Sv. The flow is clockwise around positive contours.

bottom because of the presence of NADW above AABW. The increase in salinity reaches 0.1 psu in the southern Atlantic and at depth in the southern part of the Indian Ocean, but has a typical value of 0.03 psu elsewhere.

On the other hand, the decrease in salinity caused by the enhanced sea ice melt in the open ocean in KATA is initially limited to the upper layers of the Southern Ocean. The oceanic circulation and mixing then spread this decrease, which eventually reaches all the regions that are not occupied by AABW, consistently with the conservation of salt in the World Ocean in LOVECLIM.

The AABW also displays a clear warming (not shown), of typically 0.2 °C but exceeding 0.4 °C at depth close to Antarctica. This is thought to be due to the mixing of waters originating from the shelf, during their sinking towards the deep ocean, with warmer water masses brought close to the continent by the shifts in the ACC path. Between 20° E and 80° E, where the ACC position does not change substantially, the warming at depth is due to the reduction in vertical mixing.

A comparison with observations indicates that the katabatic wind correction improves the representation of deep water properties in LOVECLIM. The right panels of Fig. 8 show that the AABW is too fresh and the NADW is too salty in the CTRL simulation. These biases are partly reduced in KATA (note that the salinity scale differs between left and right parts of the figure). Also, regionally, the improvements are noticeable. The global and annual mean absolute error in salinity decreases by 11% (from 0.14 psu in CTRL to 0.13 psu in KATA). Fig. 9, which displays the mean errors as a function of depth, shows that the KATA simulation is especially better in the deep ocean. Below 2000 m, the mean error indeed decreases by 37%.

Ocean temperatures are also in better agreement with observations when the katabatic wind correction is activated. The mean ocean temperature increases by 0.07 °C, which corresponds to a reduction in the LOVECLIM bias of around 15%. Furthermore, the global mean error decreases by 7%, and up to 9% below 1000 m, as suggested by the lower panel of Fig. 9.

## 4. Conclusions

In spite of their influence on coastal processes and on the deep ocean properties, katabatic winds are generally poorly represented in global climate models and reanalyses. The LOVECLIM model is no exception. In this study, we have tested a correction for katabatic winds and easterlies in the Southern Hemisphere to compensate for their underestimation in its atmospheric component. The corrections derive from a comparison of the mean wind stresses simulated in the vicinity of Antarctica by LOVECLIM and by a regional atmospheric model. They are constant in time, but varying in space and different in each direction. Their long-term impacts on sea ice and ocean are evaluated on the basis of two quasi-equilibrium simulations, including or not the new correction.

First, the katabatic wind correction has a significant influence on Antarctic sea ice. Along the continent and during winter, sea ice is thinner by 23%, while ice production increases by 53%. Away from the coast, the ice concentration undergoes large variations as a result of oceanic adjustments. The atmosphere plays only a passive role.

Second, the enhancement in brine rejection along the coast deeply impacts the Southern and World Oceans. The downslope flow from the continental shelf increases by 1.3 Sv and the production of AABW is higher by 2.8 Sv. Properties of AABW are also affected.

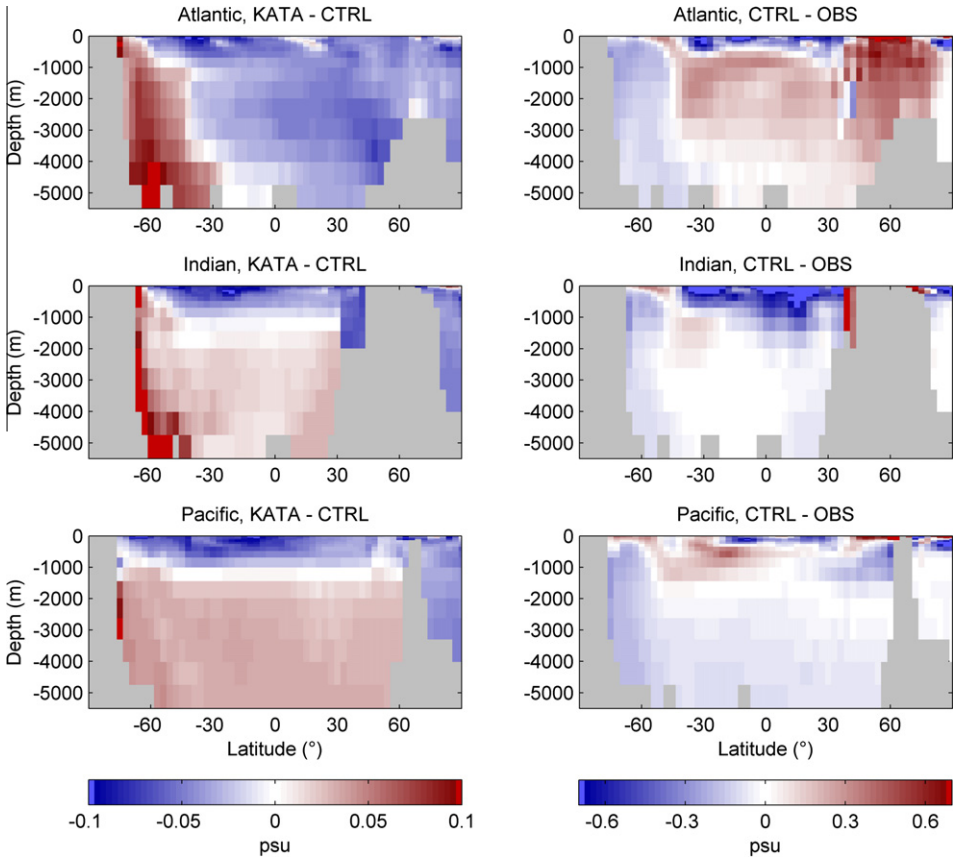


**Fig. 8.** Salinity difference (KATA–CTRL, in psu, left) and initial error on salinity (CTRL–OBS, in psu, right), in annual and zonal mean in the Atlantic (upper part), the Indian (centre part) and the Pacific (lower part) basins. For the difference, red (blue) areas correspond to higher (lower) salinity in KATA. For the error, red (blue) areas correspond to an excess (shortfall) in salinity in CTRL, with respect to observations. The salinity scale differs in each case. (For interpretation of the references to colour in this figure legend, the reader is referred to the web version of this article.)

This water mass is saltier and warmer when katabatic winds are included in the model, in better agreement with observational estimates.

The present study demonstrates the sensitivity of LOVECLIM to oceanic surface conditions in the Antarctic region. It further shows that a simple representation of coastal winds is already sufficient to significantly improve the model results at large scale. Furthermore, the correction not only reduces the large-scale biases, but also leads to improvements at the regional scale, as can be seen from the decrease in the mean absolute errors in deep ocean salinity (−37% below 2000 m) and temperature (−9% below 1000 m).

Our results have been obtained with a coarse-resolution model. In particular, the ocean model does not resolve eddies that play an important role in the dynamics of the Southern Ocean (e.g., Farneti et al., 2010; Hallberg and Gnanadesikan, 2006). Our conclusions regarding the long-term impact of katabatic winds must thus be confirmed with higher-resolution models.

However, the approach used in this study to deal with the underestimation of katabatic winds and easterlies provides an elegant way to face some common problems in ocean and climate models. It limits excessive open ocean convection in the Southern Ocean and increases the salinity of AABW and of continental shelf waters. Moreover, it obviates the need for artificial salinity enhancements around Antarctica and does not require any a posteriori tuning. We have tested it here using an intermediate complexity model, but the present resolution of coupled climate models used in the assessments made by the Intergovernmental Panel on Climate Change (IPCC; Randall et al., 2007) also prevent them to correctly simulate the katabatic flow. We thus expect that including such a correction would improve the results of those climate models too.

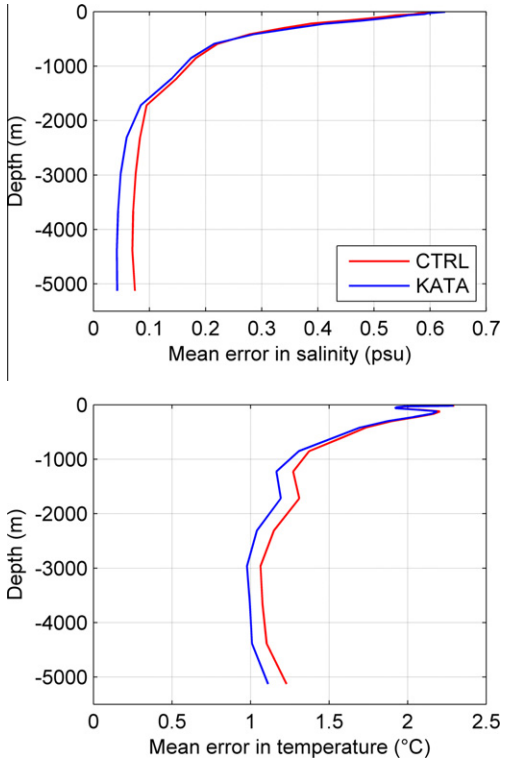


**Fig. 9.** Mean absolute error in salinity (in psu, upper part) and in temperature (in °C, lower part) as a function of depth, on an annual average, for CTRL (red) and KATA (blue). (For interpretation of the references to colour in this figure legend, the reader is referred to the web version of this article.)

## Acknowledgements

A. Barthélemy and H. Goosse are Research Assistant and Senior Research Associate with the Fonds National de la Recherche Scientifique (F.R.S. – FNRS – Belgium), respectively. This work is supported by the Belgian Federal Science Policy Office (Research Program on Science for a Sustainable Development). H. Gallée kindly provided the MAR results used in our analyses. The simulations were performed on the supercomputers of the Institut de calcul intensif et de stockage de masse (CISM) of the Université catholique de Louvain (UCL). We thank two anonymous reviewers for their valuable comments on the original manuscript.

## References

Adolphs, U., Wendler, G., 1995. A pilot study on the interactions between katabatic winds and polynyas at the Adélie Coast, eastern Antarctica. Antarctic Science 7 (3), 307–314.

Barthélemy, A., 2011. Inclusion d'une paramétrisation des vents catabatiques dans le modèle LOVECLIM. Master's Thesis, Université catholique de Louvain, Louvain-la-Neuve, Belgium, 56 pp, unpublished.

Bromwich, D.H., Kurtz, D.D., 1984. Katabatic wind forcing of the Terra Nova Bay polynya. Journal of Geophysical Research 89 (C3), 3561–3572.

Brovkin, V., Bendtsen, J., Claussen, M., Ganopolski, A., Kubatzki, C., Petoukhov, V., Andreev, A., 2002. Carbon cycle, vegetation, and climate dynamics in the Holocene: experiments with the CLIMBER-2 model. Global Biogeochemical Cycles 16 (4), 1139–1159.

Campin, J.M., Goosse, H., 1999. A parameterization of density driven downsloping flow for coarse resolution model in z-coordinate. Tellus A 51 (3), 412–430.

Conkright, M.E., Locarnini, R.A., Garcia, H.E., O'Brien, T.D., Boyer, T.P., Stephens, C., Antonov, J.I., 2002. World Ocean Atlas 2001. National Oceanographic Data Center, Silver Spring, Maryland, USA, Digital Media.

Davis, A.M.J., McNider, R.T., 1997. The development of Antarctic katabatic winds and implications for the Coastal Ocean. Journal of the Atmospheric Sciences 54, 1248–1261.

England, M.H., 1992. On the formation of Antarctic Intermediate and Bottom Waters in ocean general circulation models. Journal of Physical Oceanography 22, 918–926.

England, M.H., 1993. Representing the global-scale water masses in ocean general circulation models. Journal of Physical Oceanography 23, 1523–1552.

Farneti, R., Delworth, T.L., Rosati, A.J., Griffies, S.M., Zeng, F., 2010. The role of mesoscale eddies in the rectification of the Southern Ocean response to climate change. Journal of Physical Oceanography 40, 1539–1557.

Gallée, H., Schayes, G., 1994. Development of a three-dimensional meso-scale primitive equation model: katabatic winds simulation in the area of Terra Nova Bay, Antarctica. Monthly Weather Review 122, 671–685.

Gill, A.E., 1973. Circulation and bottom water production in the Weddell Sea. Deep-Sea Research 20, 111–140.

Goosse, H., Brovkin, V., Fichefet, T., Haarsma, R., Huybrechts, P., Jongma, J., Mouchet, A., Selten, F., Barriat, P.Y., Campin, J.M., Deleersnijder, E., Driesschaert, E., Goelzer, H., Janssens, I., Loutre, M.F., Morales Maqueda, M.A., Opsteegh, T., Mathieu, P.P., Munhoven, G., Pettersson, E.J., Renssen, H., Roche, D.M., Schaeffer, M., Tartinville, B., Timmermann, A., Weber, S.L., 2010. Description of the Earth system model of intermediate complexity LOVECLIM version 1.2. Geoscientific Model Development 3, 603–633.

Goosse, H., Deleersnijder, E., Fichefet, T., England, M.H., 1999. Sensitivity of a global coupled ocean–sea ice model to the parameterization of vertical mixing. Journal of Geophysical Research 104 (C6), 13681–13695.

Goosse, H., Fichefet, T., 1999. Importance of ice–ocean interactions for the global ocean circulation: a model study. Journal of Geophysical Research 104 (C10), 23337–23355.

Hallberg, R., Gnanadesikan, A., 2006. The role of eddies in determining the structure and response of the wind-driven Southern Hemisphere overturning: results from the Modeling Eddies in the Southern Ocean (MESO) project. Journal of Physical Oceanography 36, 2232–2252.

Jacobs, S.S., 2004. Bottom water production and its links with the thermohaline circulation. Antarctic Science 16 (4), 427–437.

Jourdain, N., Gallée, H., 2011. Influence of the orographic roughness of glacier valleys across the Transantarctic Mountains in an atmospheric regional model. Climate Dynamics 36 (5), 1067–1081.

Kim, S.J., Stössel, A., 1998. On the representation of the Southern Ocean water masses in an ocean climate model. Journal of Geophysical Research 103 (C11), 24891–24906.

King, J.C., Turner, J., 1997. Antarctic Meteorology and Climatology. Cambridge Atmospheric and Space Science Series. Cambridge University Press, Cambridge, 409 pp.

Long, M.C., Dunbar, R.B., Tortell, P.D., Smith, W.O., Mucciarone, D.A., DiTullio, G.R., 2011. Vertical structure, seasonal drawdown, and net community production in the Ross Sea, Antarctica. Journal of Geophysical Research, 116, C10029.

Massom, R.A., Harris, P.T., Michael, K.J., Potter, M.J., 1998. The distribution and formative processes of latent-heat polynyas in East Antarctica. Annals of Glaciology 27, 420–426.

Mathiot, P., Barnier, B., Gallée, H., Molines, J.M., Le Sommer, J., Juza, M., Penduff, T., 2010. Introducing katabatic winds in global ERA40 fields to simulate their impacts on the Southern Ocean and sea-ice. Ocean Modelling 35, 146–160.

Maykut, G.A., 1978. Energy exchange over young sea ice in the Central Arctic. Journal of Geophysical Research 83 (C7), 3646–3658.

Morales Maqueda, M.A., Willmott, A.J., Biggs, N.R.T., 2004. Polynya dynamics: a review of observations and modeling. Reviews of Geophysics, 42, RG1004.

Opsteegh, J.D., Haarsma, R.J., Selten, F.M., Kattenberg, A., 1998. ECBILT: a dynamic alternative to mixed boundary conditions in ocean models. Tellus A 50 (3), 348–367.

Orsi, A.H., Whitworth, T., Nowlin, W.D., 1995. On the meridional extent and fronts of the Antarctic Circumpolar Current. Deep-Sea Research I 42 (5), 641–673.

Parish, T.R., 1988. Surface winds over the Antarctic continent: a review. Reviews of Geophysics 26 (1), 169–180.

Randall, D.A., Wood, R.A., Bony, S., Colman, R., Fichefet, T., Fyfe, J., Kattsov, V., Pitman, A., Shukla, J., Srinivasan, J., Stouffer, R.J., Sumi, A., Taylor, K.E., 2007. Climate models and their evaluation. In: Climate Change 2007: The Physical Science Basis. Contribution of Working Group I to the Fourth Assessment Report of the Intergovernmental Panel on Climate Change. Cambridge University Press, pp. 589–662 (Chapter 8).

Röske, F., 2006. A global heat and freshwater forcing dataset for ocean models. Ocean Modelling 11, 235–297.

Stössel, A., Zhang, Z., Vihma, T., 2011. The effect of alternative real-time wind forcing on Southern Ocean sea ice simulations. Journal of Geophysical Research, 116, C11021.

Toggweiler, J.R., Samuels, B., 1995. Effect of sea ice on the salinity of Antarctic Bottom Waters. Journal of Physical Oceanography 25, 1980–1997.

Uppala, S.M., Kallberg, P.W., Simmons, A.J., Andrae, U., da Costa Bechtold, V., Fiorino, M., Gibson, J.K., Haseler, J., Hernandez, A., Kelly, G.A., Li, X., Onogi, K., Saarinen, S., Sokka, N., Allan, R.P., Andersson, E., Arpe, K., Balmaseda, M.A., Beljaars, A.C.M., van de Berg, L., Bidlot, J., Bormann, N., Caires, S., Chevallier, F., Dethof, A., Dragosavac, M., Fisher, M., Fuentes, M., Hagemann, S., Hólm, E., Hoskins, B.J., Isaksen, L., Janssen, P.A.E.M., Jenne, R., Mcnally, A.P., Mahfouf, J.F., Morcrette, J.J., Rayner, N.A., Saunders, R.W., Simon, P., Sterl, A., Trenberth, K.E., Untch, A., Vasiljevic, D., Viterbo, P., Woollen, J., 2005. The ERA-40 re-analysis. Quarterly Journal of the Royal Meteorological Society 131 (612), 2961–3012.

Williams, G.D., Aoki, S., Jacobs, S.S., Rintoul, S.R., Tamura, T., Bindoff, N.L., 2010. Antarctic Bottom Water from the Adélie and George V Land coast, East Antarctica (140–149°E). Journal of Geophysical Research, 115, C04027.

Zwally, H.J., Comiso, J.C., Gordon, A.L., 1985. Antarctic offshore leads and polynyas and oceanographic effects. In: Oceanology of the Antarctic continental shelf. Antarctic Research Series, vol. 43. American Geophysical Union, pp. 203–226.